

Effect of granular shape on radial segregation in a two-dimensional drum

Yue Xu(徐悦), Ran Li(李然), Zhipeng Chi(迟志鹏), Wenzheng Xiu(修文正), Qicheng Sun(孙其诚), and Hui Yang(杨晖)

Citation: Chin. Phys. B, 2024, 33 (**4**): 044502. DOI: 10.1088/1674-1056/ad1092
Journal homepage: http://cpb.iphy.ac.cn; http://iopscience.iop.org/cpb

What follows is a list of articles you may be interested in

Three-dimensional clogging structures of granular spheres near hopper orifice

Jing Yang(杨敬), Dianjinfeng Gong(宫殿锦丰), Xiaoxue Wang(汪晓雪), Zhichao Wang(王志超), Jianqi Li(李建奇), Bingwen Hu(胡炳文), and Chengjie Xia(夏成杰)

Chin. Phys. B, 2022, 31 (**1**): 014501. DOI: 10.1088/1674-1056/ac2f2f

Ultrasound wave propagation in glass-bead packing under isotropic compression and uniaxial shear

Zhi-Gang Zhou(周志刚), Yi-Min Jiang(蒋亦民), Mei-Ying Hou(厚美瑛)

Chin. Phys. B, 2017, 26 (**8**): 084502. DOI: 10.1088/1674-1056/26/8/084502

Granular packing as model glass formers

Yujie Wang(王宇杰)

Chin. Phys. B, 2017, 26 (**1**): 014503. DOI: 10.1088/1674-1056/26/1/014503

Stabilizing effect of plasma discharge on bubbling fluidized granular bed

Hu Mao-Bin (胡茂彬), Dang Sai-Chao (党赛超), Ma Qiang (马强), Xia Wei-Dong (夏维东)

Chin. Phys. B, 2015, 24 (**7**): 074502. DOI: 10.1088/1674-1056/24/7/074502

Effects of material properties on the competition mechanism of heat transfer of a granular bed in rotary cylinders

Xie Zhi-Yin (谢知音), Feng Jun-Xiao (冯俊小)

Chin. Phys. B, 2013, 22 (**8**): 084501. DOI: 10.1088/1674-1056/22/8/084501

Effect of granular shape on radial segregation in a two-dimensional drum

Yue Xu(徐悦)[1], Ran Li(李然)[1], Zhipeng Chi(迟志鹏)[1], Wenzheng Xiu(修文正)[2], Qicheng Sun(孙其诚)[3], and Hui Yang(杨晖)[4,1,†]

[1] *School of Optical-Electrical and Computer Engineering, University of Shanghai for Science and Technology, Shanghai* 200093, *China*
[2] *School of Electrical and Electronic Engineering, Shandong University of Technology, Zibo* 255049, *China*
[3] *State Key Laboratory of Hydroscience and Engineering, Tsinghua University, Beijing* 100084, *China*
[4] *College of Medical Instruments, Shanghai University of Medicine and Health Sciences, Shanghai* 201318, *China*

(Received 20 September 2023; revised manuscript received 11 November 2023; accepted manuscript online 29 November 2023)

Granular segregation is widely observed in nature and industry. Most research has focused on segregation caused by differences in the size and density of spherical grains. However, due to the fact that grains typically have different shapes, the focus is shifting towards shape segregation. In this study, experiments are conducted by mixing cubic and spherical grains. The results indicate that spherical grains gather at the center and cubic grains are distributed around them, and the degree of segregation is low. Through experiments, a structured analysis of local regions is conducted to explain the inability to form stable segregation patterns with obviously different geometric shapes. Further, through simulations, the reasons for the central and peripheral distributions are explained by comparing velocities and the number of collisions of the grains in the flow layer.

Keywords: granular materials, cubic grains, shape segregation, segregation mechanism

PACS: 45.70.–n, 45.70.Mg, 47.57.Gc **DOI:** 10.1088/1674-1056/ad1092

1. Introduction

Granular materials are complex systems formed by the interaction of many discrete solid grains with a granular size greater than 1 μm.[1,2] Ever since the Brazil nut effect was proposed, granular segregation has become a popular scientific topic.[3,4] However, most current research focuses on spherical grains and studies the influence of size and density on the segregation process and its outcomes.[5–7] In practice, a granular system generally comprises irregularly shaped grains. In nature, rocks of different shapes slide downward during mudslides. Segregation can alter the local water flow characteristics, leading to erosion of the channel bed and compromising its stability.[8] Therefore, research on segregation during landslides would significantly contribute to the prediction of geological disasters, ultimately reducing the loss of life and property. In the coal industry, mining and washing are commonly performed simultaneously. Screening of coal with different shapes is crucial as it aids in producing quality products. Thus, research on shape segregation has significant social and economic value in natural, industrial and other contexts.

Segregation of spherical grains in drums has been extensively investigated. Segregation induced by size differences is often explained by percolation mechanisms.[6,9] Segregation occurs in the direction perpendicular to the flow layer, where grains of different sizes exhibit different packing densities. There are large gaps between larger grains, which allows smaller grains to percolate through and become trapped in the center. Segregation induced by density differences is often explained by buoyancy effects.[10,11] This segregation also occurs in the direction perpendicular to the flow layer, where grains with lower density experience buoyant forces exceeding their own gravity. Thus, they float to the surface of the flow layer and are distributed around the drum. However, in shape segregation where the granular size and density are the same, the two aforementioned classical mechanisms cannot completely provide a satisfactory explanation. Thus, in-depth research is required on shape segregation.

He *et al.*[12] studied a mixture of ellipsoids and spheres at a filling degree of 40% and observed that alterations in the aspect ratio of the grains caused spherical grains to inconsistently concentrate in the center. They suggested that changes in the aspect ratio could lead to variations in the void size on the flow layer surface, thereby affecting the segregation results. Dube *et al.*[13] conducted simulations of cylindrical grains and reached a conclusion opposite to that of traditional segregation results where smaller grains were observed to be distributed around the periphery. They inferred that the segregation of the two types of cylindrical grains was determined by their base widths. Claudia *et al.*[14] mixed spherical and ellipsoidal grains with the same volume; they observed that increases in the aspect ratio of ellipsoidal grains decreased their rolling ability, causing them to become trapped in the center of the drum. Thus, the factors affecting the segregation of spherical and differently shaped grains are not the same. With re-

[†]Corresponding author. E-mail: yangh_23@sumhs.edu.cn

© 2024 Chinese Physical Society and IOP Publishing Ltd

spect to the segregation of spherical and typical non-spherical grains, such as block-like grains, Pereira *et al.*[15] conducted simulations and indicated that from the perspective of energy dissipation, the sharpness of granular edges led to the differences in energy consumption, resulting in segregation. The sharp edges of block-like grains increased the degree of segregation. Lu *et al.*[16] used simulations to explain segregation in terms of mobility and the number of granular collisions. They observed that the change of the segregation degree between block-like grains with different edge angles and spherical grains was relatively small. A comparison of the simulation results from Pereira *et al.* and Lu *et al.* revealed that there is a low degree of segregation due to the effect of shape. However, the radial distribution continues to be contentious, and most existing research is based on simulations only. Therefore, previous studies suffer from limitations and further experiments are required to address this issue. The achievement of a universally accepted and consistent result for shape segregation of spherical and cubic grains remains a challenge. This study identifies the segregation phenomena of cubic and spherical grains via experiments and provides explanations from experimental and simulation perspectives.

2. Method

2.1. Experimental apparatus and grains

Figure 1 shows the experimental setup for granular segregation. The experimental apparatus comprises a drum, a motor system, a complementary metal–oxide–semiconductor (CMOS) high-speed camera and a light-emitting diode (LED) light source. During the experiment, the LED light source is directed toward the drum and the CMOS high-speed camera is used to continuously capture images of the grains. The drum is made of processed organic glass with a diameter of 150 mm and an adjustable depth range of 0–250 mm. To ensure that the system only produces radial segregation, the drum depth is adjusted to 20 mm during the experiment, with a filling degree of 50% and a rotation speed of 5 rpm. A high-speed camera (Revealer 3F04M) is aimed at the drum, which continuously captures images. The images are collected and processed by a computer with a sampling interval of 10 ms. To avoid interference from reflected light in image acquisition, the LED light source (SL-200W) is positioned at an angle of $45^\circ \pm 5^\circ$ relative to the drum with an output power of 200 W. The materials and shapes of the grains are important parameters. Three types of grains are used in the study; their parameters are listed in Table 1. Given the difficulty in identifying and distinguishing two transparent grains in images captured by the high-speed camera, ten random grains of type B are painted black to track the changes in their positions to study the distribution.

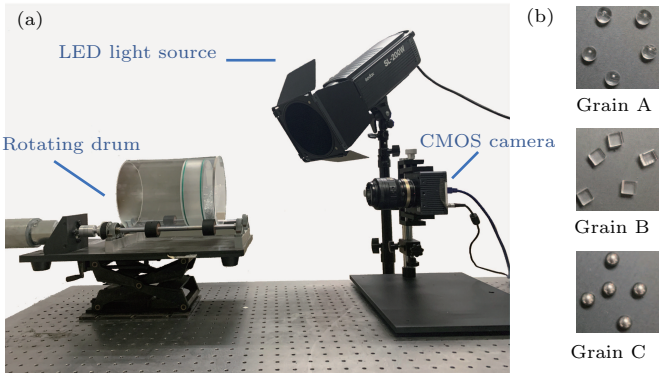


Fig. 1. System and grains: (a) segregation experiment setup; (b) grain A: spherical PMMA, grain B: cubic PMMA, grain C: spherical stainless steel.

Table 1. Grain parameters.

Grain	Material	Shape	Density (g/cm^3)	Size (mm)
A	PMMA	sphere	1.2	3
B	PMMA	cube	1.2	3
C	stainless steel	sphere	7.93	3

2.2. Discrete element method

Segregation can be studied using a discrete element method (DEM) model with Hertz–Mindlin contact forces, allowing real-time tracking of grain motion while considering the interactions between grains and between grains and boundaries.[17,18] The translation and rotation motion of grains are described using Newton's second law of motion. For grain i, interaction with grain j can be expressed as follows:

$$m_i \frac{\mathrm{d}u_i}{\mathrm{d}t} = \sum_{j=1}^{n} \left(F_{\mathrm{cn},ij} + F_{\mathrm{dn},ij} + F_{\mathrm{ct},ij} + F_{\mathrm{dt},ij}\right) + G_i, \quad (1)$$

$$I_i \frac{\mathrm{d}\omega_i}{\mathrm{d}t} = \sum_{j=1}^{n} \left(T_{\mathrm{t},ij} + T_{\mathrm{r},ij}\right), \quad (2)$$

where u_i, ω_i and I_i denote translational velocity, angular velocity and moment of inertia of grain i, respectively. Furthermore, $F_{\mathrm{cn},ij}$ and $F_{\mathrm{ct},ij}$ denote normal and tangential contact forces between grains i and j, respectively; $F_{\mathrm{dn},ij}$ and $F_{\mathrm{dt},ij}$ denote the normal and tangential damping forces between grains i and j, respectively; and G_i denotes the gravity acting on grain i. The torque acting on grain i is generated by tangential forces and rolling friction forces, denoted as $T_{\mathrm{t},ij}$ and $T_{\mathrm{r},ij}$, respectively. The forces and torques correspond to the sums of n grains in contact with grain i.

This method is used to simulate mixing of grains A and B. The drum is a cylindrical vessel with a diameter of 150 mm and a thickness of 20 mm. The elongated cylinder is modeled using periodic boundary conditions and neglecting axial segregation. Gravity acts in the negative y-direction. The spherical grains exhibit a diameter of 3 mm. The cubic grains are modeled using a sphere-packing method where 27 spherical grains are connected to each other and overlap to form a cubic grain. Each small sphere has a diameter of 1.5 mm. The distance between the centers of the spheres is 0.75 mm and results in a

cubic grain with a side length of 3 mm. The spherical grain at the center of each cubic grain is referred to as the host grain and the 26 surrounding grains are referred to as subordinate grains. For each cubic grain, only subordinate grains are used to represent the geometric contours of the cubic grain. The material properties and motion information of the cubic grains are represented by the central host grain, including attributes such as mass, material properties, spatial orientation and center-of-mass position of the cubic grain. Collisions between cubic grains can be transformed into binary collisions between subordinate grains. Using the same approach, any edge-to-edge, wall-to-wall or edge-to-wall contact between cubic grains can be transformed into a spherical grain-to-spherical grain contact. To simplify the problem and improve computational efficiency, a restitution coefficient of 0.1 is set in the simulation. The other system parameters used for the DEM simulations are listed in Table 2.

Table 2. Numerical parameters in the simulations.

Parameter	Value
Grain density (kg/m^3)	1200
Grain A diameter (mm)	3
Grain B side length (mm)	3
Grain number (A and B)	3183 and 1926
Shear modulus (Pa)	2.1×10^8
Poisson's ratio	0.29
Restitution coefficient between grain–grain, grain–wall	0.1
Static friction coefficient between grain–grain, grain–wall	0.8
Rolling friction coefficient between grain–grain, grain–wall	0.02

The simulation is designed to explain certain phenomena in the experiments and it is consistent with the experimental conditions. Preprocessing is performed prior to the simulation. Two sector-shaped containers are created, each with an area equivalent to one-quarter of the drum surface and a thickness matching the drum depth of 20 mm. The containers are filled with cubic and spherical grains. The numbers of spherical and cubic grains required to fill one-quarter of the container are 3183 and 1926, respectively. The grains are randomly generated from the top of the drum at an initial velocity of 2 m/s. After loading is completed, the filling degree of the system is approximately 50%. Figure 2 shows the typical trajectories of the two grains with different shapes. Specifically, I represents the initial position and II represents the final position. Spherical grains start near the edges and eventually stabilize in the center. Cubic grains start in the center and eventually stabilize near the edges. The segregation results show that spherical grains are located in the center and cubic grains are located near the edges. This is consistent with the distribution observed in the experimental results.

To examine the velocities of the different grains within the flow layer of the simulation system, the drum surface is divided into nine perpendicular rectangular containers of the same size, with a length of 15 mm (five times the granular diameter), width of 15 mm and height of 50 mm to cover the entire flow layer. The maximum velocities of the top ten grains of each shape in each rectangular container are separately calculated. The average velocities of 90 grains of each shape are determined and the frequencies of the different velocities are recorded.

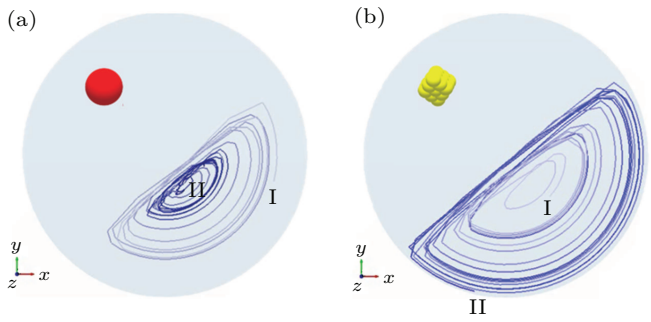


Fig. 2. Typical grain trajectories: (a) spherical grain; (b) cubic grain.

2.3. Degree of segregation

The quantification of the degree of segregation uses the segregation index I_S,[16]

$$I_S = \sqrt{\frac{\sum_{k=1}^{N_c} (f_k - \bar{f})^2}{N_c - 1}}, \tag{3}$$

where N_c denotes the total number of grids, f_k denotes the proportion of a certain type of grain in the kth grid and $\bar{f}$ denotes the average proportion of a certain type of grain in k grids. A value of 0.5 indicates more thorough segregation and a value approaching 0 suggests a higher degree of mixing. The drum is divided into several equal-sized grids wherein each displays a length and width equal to five times the granular diameter. Figure 3 shows the variation curve for the segregation index I_S in the DEM, which can be divided into three stages.

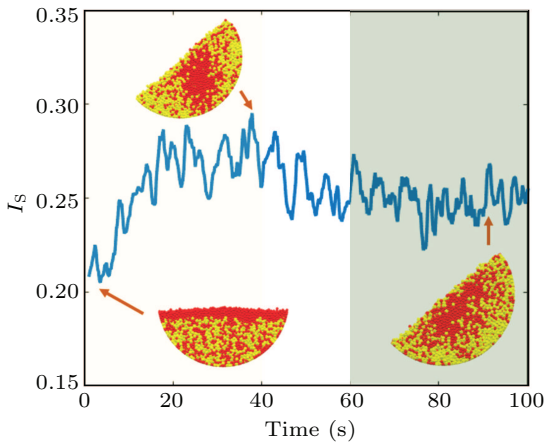


Fig. 3. Evolution of the segregation process.

Initially, the mixing index is relatively low (approximately 0.2), indicating a higher degree of mixing. The volume ratios of the grain types are identical to ensure consistency between the simulated and experimental systems. The number of spherical grains exceeds the number of cubic grains and there is a top layer of spherical grains. This results in an initial state that is not a complete mixture and a numerical value that is not zero. Within 0–40 s, the overall trend of I_S increases and reaches a peak of 0.3. This is because the top layer of spherical grains briefly aggregate while rolling, resulting in a relatively high degree of segregation when the spherical grains have not yet dispersed. After 60 s, the granular system stabilizes and the I_S remains at approximately 0.25, indicating a relatively high degree of mixing and shape segregation.

3. Results and discussion

3.1. Experiment results

Figure 4 shows a superimposition of 2000 consecutive images of tracked grains acquired in the experiment after the segregation system is stabilized. For ease of observation and analysis, the images undergo rotation, color change, binarization and opening and closing operations. Figure 4(a) shows the inverted-color-processed result; the white areas indicate the distribution positions of the tracked grains within 20 s. It is observed that the tracked cubic grains are mainly distributed around the granular system after the segregation system is stabilized, with no cubic grains in the center. Figure 4(b) shows the normalized results where darker colors indicate a higher frequency of tracked grains at that position. The figure shows seven small white squares in the center, indicating the absence of cubic grains in the central area, which accounts for 5.6% of the calculated region. The volume ratio of the grains loaded into the system is identical. Only a small portion of the center lacks cubic grains, indicating incomplete segregation based on the shapes of the spherical and cubic grains.

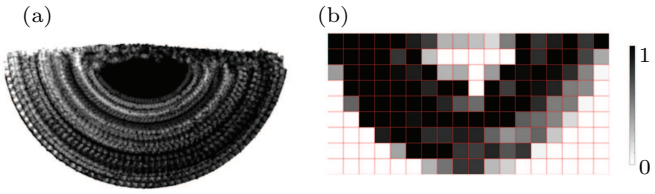


Fig. 4. Distribution of tracked grains: (a) inverted-color-processed result; (b) normalized result.

3.2. Segregation results for three grain combinations

Figure 5 depicts two additional comparative experiments based on shape segregation. Each experiment involves two types of grain with equal volume, resulting in a filling degree of 50%. Grains A and C form a typical experimental density segregation system, where the buoyancy effects lead to segregation in a direction perpendicular to the flow layer. Heavier stainless-steel grains gather in the center whereas lighter PMMA grains are distributed around the periphery, creating a distinct segregation boundary, indicated by the red marks in Fig. 5. This experimental phenomenon is consistent with previous findings and conclusions.[19,20] A comparative experimental group composed of grains B and C is established to investigate the influence of adding the shape factor to density segregation. The experimental pattern of B+C in Fig. 5 shows relatively clear segregation with yellow lines marking the boundary between the two types of grains. Although the

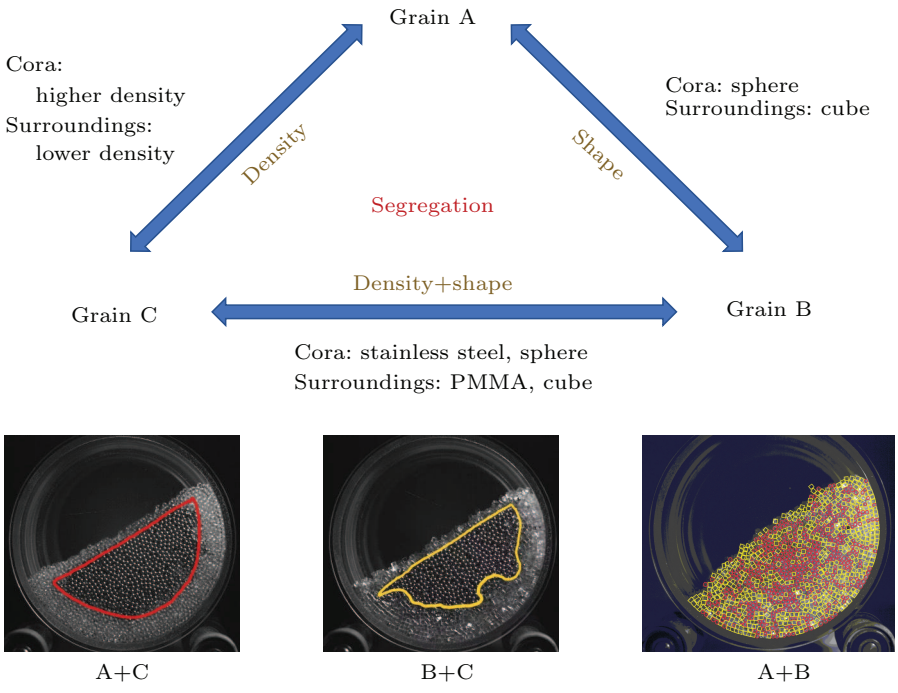


Fig. 5. Segregation of the three grain combinations.

segregation between grains B and C are mainly determined by buoyancy effects due to the differences in density, the presence of shape factors competes with the density and this results in irregular protrusions in the segregation locations of the two grain types. The combination of grains A and B eliminates the effect of density and the segregation results are determined by the granular shape. Cubic grains are denoted in yellow and spherical grains are denoted in red. As shown in Fig. 5, for A+B, the segregation pattern does not exhibit distinct boundaries.

To further investigate the effect of shape factors on segregation, a local analysis of the segregation results for grains B and C is conducted. During the descent of these grains, cubic grains form relatively stable clusters at the top of the flow layer that can persist for a time, as shown in Fig. 6(a). The relatively stable clusters begin to descend when the drum continues to rotate. Cubic grains carry more grains as they fall along the flow layer. Particle image velocimetry is used to analyze grain velocities in the flow layer and reveals that, when compared with density segregation, the addition of shape factors increases the thickness of the flow layer. Density segregation can drive approximately three layers of grains to flow in the center of the flow layer. However, with the added effect of shape factors, it can carry up to approximately six layers of grains in the center. The thicker the flow layer in the segregation system, the more energy it possesses during descent. This allows some spherical grains to reach lower positions and disrupt the boundaries of the existing cubic grains. This leads to irregular protrusions, as shown in Fig. 6(b). When the effect of density is completely eliminated, only the effect of the granular shape remains and the boundary between the two types of grains is disrupted to a greater extent, resulting in a lower degree of segregation.

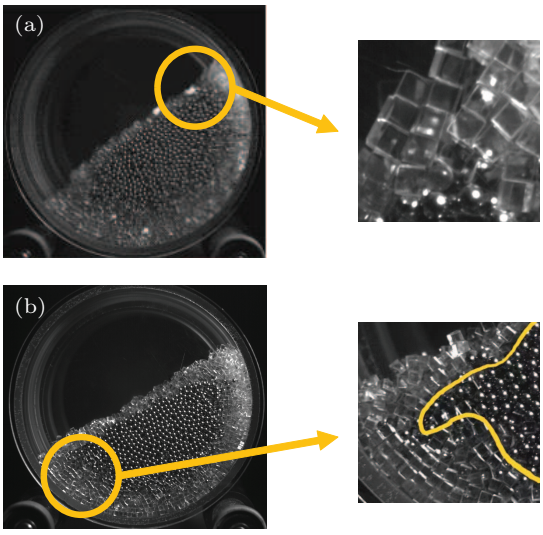


Fig. 6. Local changes during evolution of segregation: (a) stable clusters at top of the flow layer; (b) disrupted boundary.

3.3. Velocity and collision in the flow layer

Figure 7(a) presents the cubic and spherical grain velocities in the simulation for a time interval of 90–100 s, with data collected every 0.2 s. Velocities ranging from 0.13 m/s to 0.28 m/s are divided into ten intervals, in increments of 0.015 m/s. The number of occurrences of different velocities in the ten intervals is calculated and a Gaussian curve is used for fitting. The graph shows that the average velocity of the cubic grains is approximately 0.24 m/s and the average velocity of the spherical grains is approximately 0.18 m/s. Cubic grains exhibit greater velocity than spherical grains and this allows them to reach the bottom of the flow layer more quickly during descent. The variances in the velocities of the cubic and spherical grains are similar, thereby indicating similar velocity fluctuations.

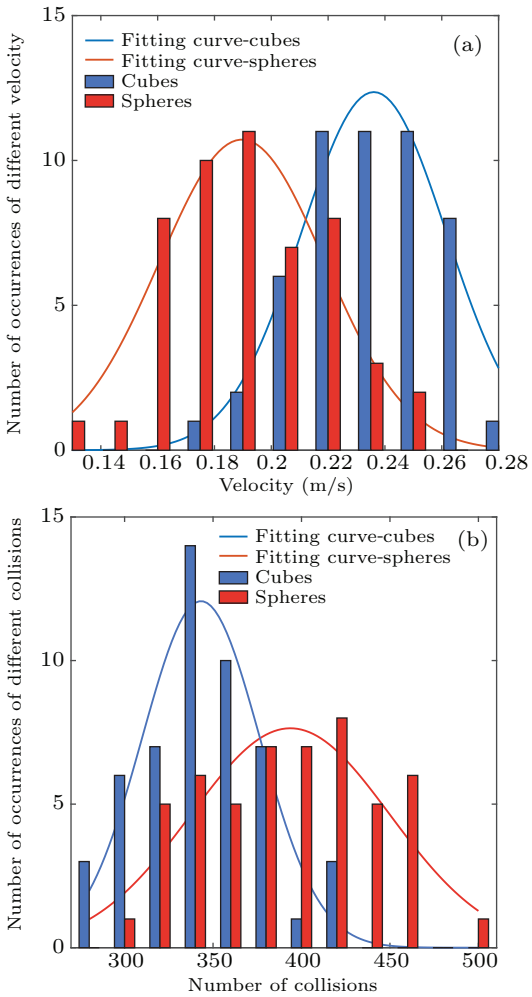


Fig. 7. Characteristics of grains in the flow layer: (a) velocity; (b) collision frequency.

When the grains enter the passive layer, they undergo a rigid motion with the drum. Rolling occurs upon reentry into the flow layer. More collisions during descent indicate greater energy dissipation, leading to shorter rolling distances. Figure 7(b) illustrates the collisions between the two types of grains. Collisions are recorded at intervals of 0.2 s in a period from 90 s to 100 s, yielding 51 datasets. Collision counts are grouped into 11 intervals where each spans 20 collisions and ranges from 280 to 500. The frequency of occurrence in these 11 intervals across 51 datasets is calculated and fitted using Gaussian curves. The graph shows that the average colli-

sion count for cubic grains is approximately 350, whereas the average collision count for spherical grains is approximately 390. This indicates that the spherical grains experience greater energy dissipation during their motion, resulting in shorter rolling distances. Consequently, spherical grains tend to accumulate in the center whereas cubic grains roll farther due to fewer collisions and are distributed around the periphery. However, the variance of collision counts for cubic grains exceeds that for spherical grains and indicates that the collision counts of cubic grains fluctuate more and are relatively dispersed compared to those of spherical grains.

Analysis of the velocity and collision frequency of the grains in the flow layer demonstrated why the spherical grains are prone to accumulate at the center, whereas cubic grains are distributed around them.

3.4. Influence of volume ratio on segregation results

In industry, the proportion of mixed grains is an important consideration during the loading process. Grains A and B are mixed with different volume ratios to study the influence of volume ratio on shape segregation. Figure 8 shows the normalized segregation results for cubes : spheres = 3:7 and 7:3 with cubes mostly distributed around the periphery and spherical grains are concentrated in the center. As shown in Figs. 4(b) and 8, for the three ratios, there are 10, 7 and 4 grids in the central area, which are white. This indicates that with an increase in the proportion of cubic grains, the available area in the center where the spherical grains arrive decreases. When the proportion of cubic grains reaches 70%, the aggregation area of the spherical grains in the center is only 3% and is significantly less than the overall proportion of 30%. This indicates that segregation between the cubic and spherical grains is incomplete and that the shape factor disrupts the segregation pattern. The rotation speed of the drum also affects segregation. The adjustable range of the rotational speed is 0–0.612 rad/s. I_S increases when the rotation speed of the drum increases. When the speed exceeds 0.55 rad/s, the I_S does not change significantly.

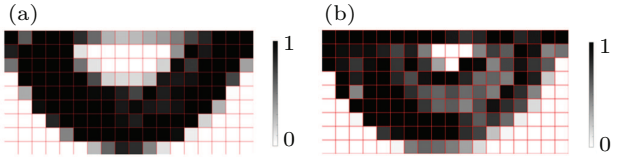


Fig. 8. Segregation results with different volume ratios: (a) cubes : spheres = 3:7; (b) cubes : spheres = 7:3.

4. Conclusion

Segregation of cubic and spherical grains is studied via establishment of an experimental platform and simulations. The following observations and possible explanations can be obtained:

When the rotation speed is 5 rpm, the segregation results for both cubic and spherical grains indicate that the spherical grains gather in the center and cubic grains distribute around them. The radial distribution is not affected by changes in the volume ratio. Moreover, compared to size and density segregation, the degree of segregation is lower and stable segregation patterns with significant geometric shapes cannot be produced in the shape segregation process. First, the evolution of the degree of segregation demonstrates the incompleteness of shape segregation. The reasons for the disruption of boundaries are presented from a structural perspective via segregation of the three types of grains. The cubic grains form relatively stable clusters at the top of the flow layer and roll together. During their descent, they carry more spherical grains, thereby leading to an increase in the thickness of the flow layer compared with that observed in density segregation. Thus, they possess more energy during their descent. Some spherical grains reach further positions and disrupt the boundaries of the original cubic grains, resulting in irregular protrusions and destruction of the original core segregation patterns. Then, the velocity and the number of granular collisions of the two types of grains in the flow layer are calculated in simulations to explain why spherical grains gather at the center and cubic grains are distributed around them. The typical granular trajectories also confirm this distribution.

Acknowledgement

Project supported by the National Natural Science Foundation of China (Grant Nos. 12072200 and 12372384).

References

[1] Zhu H P and Yu A B 2007 *Chem. Eng. Sci.* **62** 3378
[2] Mondal C, Moshe M, Procaccia I, Roy S, Shang J and Zhang J 2022 *Chao. Soliton Fract.* **164** 112609
[3] Liu Y, Wang C and He C 2022 *Powder Technol.* **401** 117350
[4] Peng Y J, Zhang Z, Wang Y and Liu X S 2012 *Acta Phys. Sin.* **61** 134501 (in Chinese)
[5] Gray J M N T, Gajjar P and Kokelaar P 2015 *CR Phys.* **16** 73
[6] Xiu W Z, Li R, Chen Q, Sun Q C and Yang H 2021 *Powder Technol.* **380** 518
[7] Tunuguntla D R, Weinhart T and Thornton A R 2017 *Comput. Part. Mech.* **4** 387
[8] Jing L, Kwok F C Y, Zhao T and Zhou J W 2018 *4th GeoShanghai International Conference on Geoenvironment and Geohazard*, May 27, 2018, Shanghai, China
[9] Arntz M M H D, Otter W K D, Briels W J, Bussmann P J T, Beeftink H H and R M Boom 2008 *AIChE J.* **54** 3133
[10] Pereira G G, Sinnott M D, Cleary P W, Liffman K, Metcalfe G and Šutalo I D 2011 *Granular Matter* **13** 53
[11] Liao C C, Hsiau S S and Nien H C 2014 *Phys. Rev. E* **89** 060001
[12] He S Y, Gan J Q, Pinson D and Zhou Z Y 2019 *Powder Technol.* **341** 157
[13] Dubé O, Alizadeh E, Chaouki J and Bertrand F 2013 *Chem. Eng. Sci.* **101** 486
[14] Claudia P, Marco M, Colin H, Andrea C S and Marco R 2018 *Proceedings 8th World Congress on Particle Technology*, April 22, 2018, Orlando, America
[15] Pereira G G and Cleary P W 2017 *Granular Matter* **19** 23
[16] Lu G and Müller C R 2020 *Granular Matter* **22** 50
[17] Wang W G, Zhou Z G, Zong J and Hou M Y 2017 *Chin. Phys. B* **26** 242
[18] Chen P Y, Jia F G, Han Y L, Meng X Y, Li A Q, Chu Y H and Zhao H W 2022 *Powder Technol.* **404** 117393
[19] Liao C C, Hsiau S S and Nien H C 2015 *Powder Technol.* **284** 514
[20] Liao C C, Hsiau S S and Wen S F 2016 *Adv. Powder Technol.* **27** 1265